Persistent Scatterers Time Series Fusion with Datasets from Several Periods

Yu-Heng Tai[1*], Fuan Tsai[1], Chung-Pai Chang[1]

[1]Center for Space and Remote Sensing Research, National Central University

constantinevi@outlook.com

Abstract *Interferometric Synthetic Aperture Radar (InSAR) technology, especially Persistent Scatterers InSAR (PSInSAR), has become a general tool for monitoring large-scale, long-term surface deformations. It is extensively used in earthquake research, land subsidence monitoring, and volcano risk management. These methods require strict qualification on phase signal processing from SAR data, asking for images from the same satellite system, orbit, and acquisition mode. However, the finite lifespan of satellites limits the duration of PSInSAR analysis to the satellite's operational period. Once a satellite is decommissioned, PSInSAR observations cease, and combining datasets from different satellite systems is challenging due to system inconsistencies. This study presents a novel approach to merge two PSInSAR datasets from different SAR missions with a short overlap period. By correcting system biases arising from various reference points in the temporal domain, we create a new, long-period fusion PSInSAR dataset from two shorter-period datasets. This enables time series analysis across datasets from different satellite systems. The fusion dataset is compared with the datasets, with similar monitoring periods, generated from the conventional method, showing consistent deformation trends and validating the feasibility of this method for deformation analysis and GIS applications. This fusion approach mitigates the risks associated with satellite operational lifespans, extending the utility of InSAR technology for long-term monitoring applications.*

Keywords: *SAR, Persistent Scatterers, Time series*

Introduction

Differential Interferometric Synthetic Aperture Radar (DInSAR) has become a widely used geodetic monitoring tool. Using spaceborne radar systems, DInSAR technology emits radar waves toward the Earth's surface and receives the returning echoes, thereby acquiring information on the intensity and phase of these surface reflections. Satellites operating in sun-synchronous orbits enable periodic imaging of a specific location, providing a continuous time series of radar images for that area. By performing differential interferometry on two images acquired at different times, it is possible to derive the phase difference due to changes in the distance to the target over the acquisition period, thereby calculating the amount of surface deformation (Massonnet et al., 1998). SAR is an active sensing technique that does not rely on sunlight reflection, allowing effective measurement even at night. With wavelengths longer than visible light, radar waves offer superior penetration capability, enabling them to pass through clouds, fog, and dust to reach the surface and return to the satellite with minimal interference from weather or haze. Additionally, radar remote sensing provides surface information over

large areas, enabling estimation of relative displacements in the surveyed region with centimeter-level accuracy, which is challenging to achieve using other measurement techniques. Advanced methods like Persistent Scatterer Interferometry Synthetic Aperture Radar (PSInSAR), developed by A. Hooper (Hooper et al., 2004), have been successfully applied to observe surface deformations in various cases, including volcanoes (Antonielli et al., 2014), earthquakes (Chini et al., 2010), fault activity (Huang et al., 2016), and land subsidence (Le et al., 2016). With the development of ultra-high-resolution radar satellites, DInSAR technology has increasingly been applied to monitor specific structures, such as buildings, engineering structures, dams (Milillo, 2016), and transmission towers (Luo et al., 2014).

However, a stringent requirement is necessary for processing the phase signals from radar images. Images used in differential interferometry must be acquired from the same satellite system, with identical orbit, band, and acquisition mode. Consequently, images from different satellites, acquisition modes, or bands cannot be used for interferometric processing. Although there are numerous active radar satellite systems, different satellite systems often carry radar sensors with varying bands, and their orbits and imaging modes are also distinct. As a result, it remains challenging to integrate and compare results calculated from different satellite data. Furthermore, satellites are limited by lifespan, meaning they cannot perform missions indefinitely. Different satellite missions generally cover distinct observational timeframes, with most common satellite missions targeting five-year durations and some extending to seven to ten years. However, the performance and expected lifespan of future satellite instruments are not guaranteed, limiting the maximum monitoring period for surface deformation to around five years. Ensuring continuity in long-term observations is one of the challenges phase of PSInSAR technology.

In this study, a technique, named “PSInSAR Dataset Fusion”, for fusing persistent scatterer interferometry results, enabling long-term monitoring by incorporating images from different time intervals and radar satellites, is developed. When applying the fusion technique for interferometric results of two datasets from different time intervals or different radar sources, the datasets must overlap to a certain extent. Using persistent scatterer data from the overlapping period allows for data alignment, reducing or eliminating systematic errors arising from differences in reference points in the temporal

domain. This process produces a combined time series for interferometric analysis across two datasets with different periods.

Methodology

This section describes the methodology of PSInSAR dataset fusion in detail. This procedure aims to combine the time series of a single target across two datasets with different periods. The main concept of time series fusion is presented in Figure 1. A bias between two timeseries, caused by the difference of start point in the temporal domain, is displayed. To remove this bias and merge time series, the fusion procedure is developed. The workflow is illustrated in Figure 2.

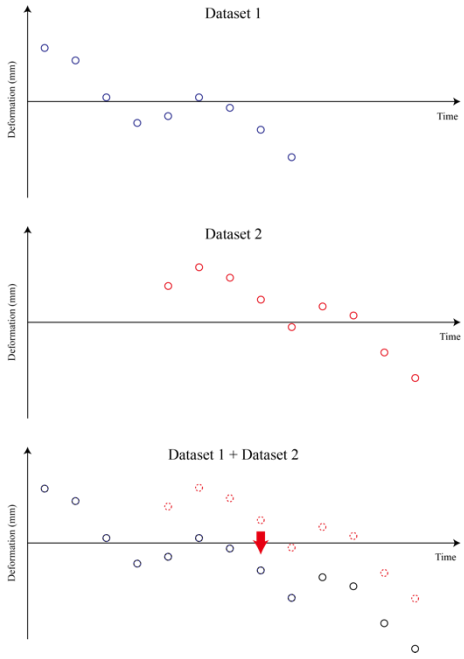

Figure 1: The main concept of time series fusion.

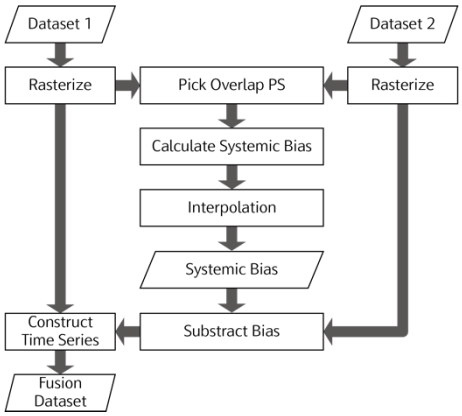

Figure 2: The main concept of time series fusion.

The PSInSAR results consist of point data, where the coordinates of Persistent Scatterer (PS) pixels are derived from the master image in the differential interferometry processing. When different master images are used during the image processing, the final positions of PS points may have a slight difference. Therefore, when fusing the time series of two datasets, it is expected that the positions of PS points will differ between datasets. Additionally, in the second phase, where time series fusion involves different sensors, there will be discrepancies in spatial resolution between the two datasets. Therefore, a translation of PS from point cloud to raster could help harmonize the spatial resolution of the two sets of results. In this study, rasterization using the near neighbor method is performed by defining a grid based on a selected starting point within the target area. The grid resolution is set depending on the spatial resolution of different SAR images. To preserve the nature of the PSInSAR point data, this procedure is used to search for and fill in PS deformation within each grid cell, while grid cells without PS points are assigned no-data values. The final output is a grid dataset of PS pixels in GeoTiff format.

Since the two datasets may contain different PS pixels, a step involves selecting the PS pixels that existed in the two datasets, i.e., the continuous PS pixels after gridding. These continuous PS pixels serve as the basis for subsequent analysis, establishing temporal correlations between the two datasets and ensuring continuity in the fusion dataset.

After rasterization, linear regression is applied to the overlapping period between the two datasets to calculate the systematic bias between the two datasets. This bias serves as a reference for adjusting the time series data in subsequent steps (see Figure. 3).

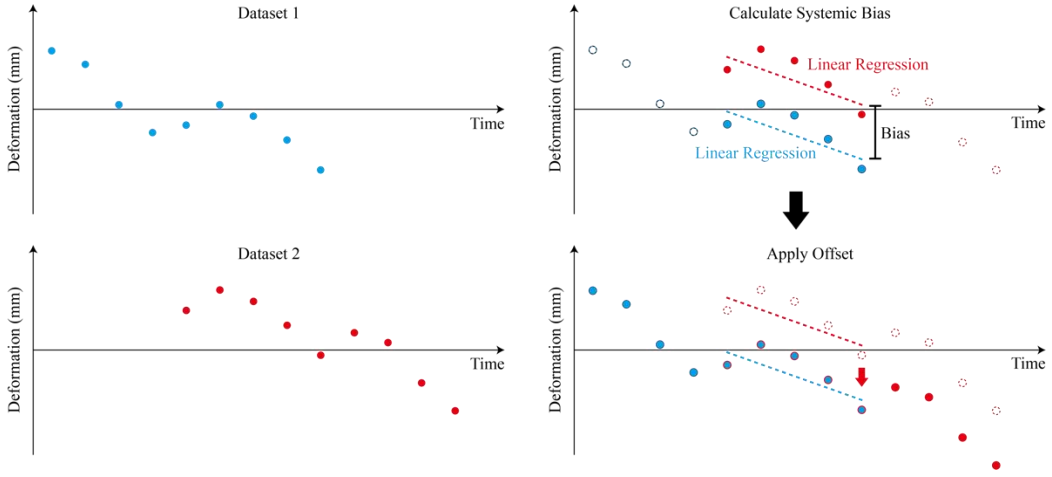

Figure 3: The procedure of calculating bias between time series.

For those PSs that don't exist in both datasets (i.e. uncontinuous PS), the bias can not be obtained, resulting in being abandoned before. In this stage, we introduce an additional step by applying the interpolation to the bias from continuous PS to acquire the offset for

these uncontinuous PSs (see Figure. 4). Triangulated Irregular Network (TIN) method is selected for spatial interpolation of the systematic offset across continuous PS points. Compared to the Inverse Distance Weighting (IDW) method, TIN offers computational efficiency and ensures interpolation coverage within the triangular network, achieving the objective of maximizing the retention of uncontinuous PS. This interpolated offset is applied to each uncontinuous PS to reconstruct the time series for all PS points in all datasets.

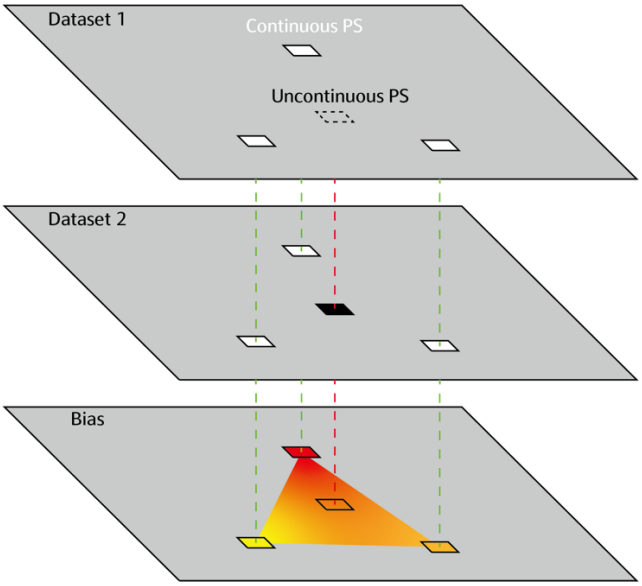

Figure 4: The interpolation is applied to obtain bias for uncontinuous PSs.

After the interpolation, subtract the systematic offset calculated in the previous step from the gridded PS pixel data. This process allows the integration of non-overlapping parts of the two datasets, thereby extending the multi-period deformation monitoring results of PSInSAR. Finally, all adjusted time series data are exported, yielding the fusion dataset.

Study Area

The selected study area is located in the Yunlin County region of Taiwan, known for experiencing significant and continuous land subsidence. As illustrated in Figure 5, long-term monitoring data reveal a persistent subsidence trend in this region, primarily driven by extensive groundwater extraction for agricultural and industrial purposes. Yunlin's geological characteristics, combined with ongoing human activities, have made it one of Taiwan's most prominent subsidence zones.

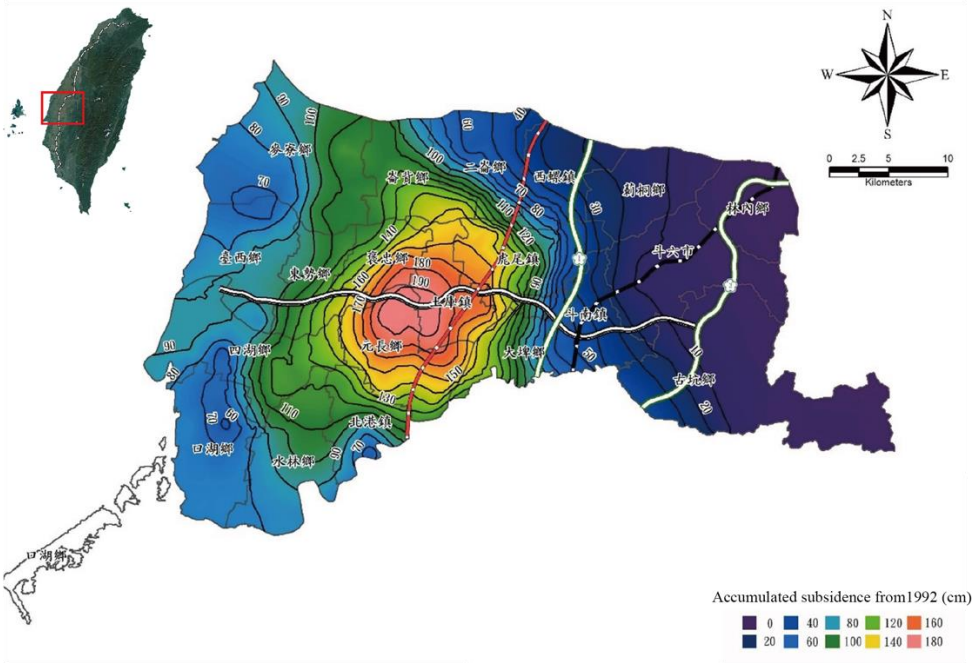

Source: Water Resources Agency, Taiwan

Figure 5: The accumulated subsidence of the Yunlin area.

This area is particularly suitable for the development and testing of the proposed fusion technique for PSInSAR datasets, as it has consistent coverage of both Sentinel-1 and TerraSAR-X satellite imagery. The availability of these two satellite datasets provides a unique opportunity to fuse the time series data across different satellite missions, enhancing the temporal coverage and continuity of surface deformation monitoring. Sentinel-1, with its high temporal resolution, enables regular monitoring of surface deformation, while TerraSAR-X provides high spatial resolution, allowing for more detailed observations within the region. The integration of these datasets allows for a comprehensive analysis of subsidence patterns.

Furthermore, the region is densely covered by a network of Global Navigation Satellite System (GNSS) stations, which provides an independent source of precise ground displacement data. This GNSS network serves as a valuable validation tool, allowing for the cross-verification of the fusion PSInSAR results and ensuring the reliability of the fusion method in accurately capturing long-term deformation trends across datasets. The abundance of satellite imagery and ground-based GNSS data makes Yunlin an ideal study area for validating the effectiveness and accuracy of the proposed PSInSAR fusion technique.

Data

This study employs imagery acquired by the Sentinel-1 and TerraSAR-X satellite for development. Sentinel-1 is part of the European Space Agency's (ESA) Copernicus Program, an ambitious satellite initiative aimed at creating a global environmental monitoring network. Sentinel-1A was successfully launched in April 2014 and began delivering Single Look Complex (SLC) images covering Taiwan in October 2014, while Sentinel-1B followed with its launch in April 2016. On the other hand, TerraSAR-X, an X-band radar satellite, developed and launched by the German Aerospace Center (DLR), currently operates as a constellation of three satellites: TerraSAR-X (launched in 2007), TanDEM-X (launched in 2010), and PAZ (launched in 2018). These satellites are operated by Airbus Defense and Space and offer a maximum revisit period of 11 days. TerraSAR-X is capable of imaging in a specialized Staring Spotlight mode, which achieves a resolution as fine as 25 cm, though with a limited coverage area of 4x4 km, making it ideal for focused target monitoring.

We also applied to the Ministry of the Interior, Taiwan, for time series observational data from the Global Navigation Satellite System (GNSS) continuous stations. Taiwan has one of the highest densities of GNSS stations in the world, with over 500 continuous stations across the island. These stations are established and maintained by organizations such as the Central Geological Survey, the Central Weather Bureau, and Academia Sinica. They provide daily three-dimensional observation to compare with PSInSAR results, GNSS data will be re-project to the radar line of sight (LOS) according to the satellite orbit information, the LOS mean velocity is shown in Figure 6. In addition, to ensure that the comparison between every result has the same reference point, GNSS and PSInSAR results will use GNSS station CHSG as a reference point in the spatial domain.

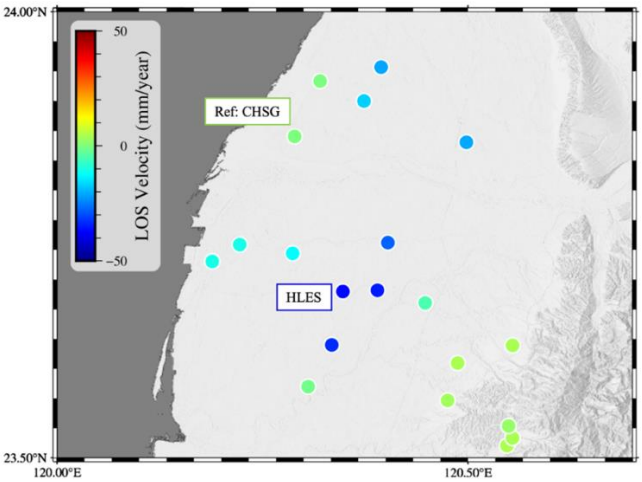

Figure 4: Mean velocity of GNSS station in LOS direction in the study area.

In the first phase of this study, we utilized Sentinel-1 images from 2014 to the end of 2017, amounting to a total of 55 images over three years. The images were processed using PSInSAR techniques and divided into three data subsets. The first subset, spanning from November 2014 to the end of 2016, comprises 32 images, while the second subset, from January 2016 to the end of 2017, includes 38 images. A third dataset, comprising all 55 images from 2014 to 2017, serves as a reference set. Additionally, GNSS station data were collected to verify the accuracy and precision of the fusion method.

The second phase of this research involved fusing datasets from TerraSAR-X and Sentinel-1 to evaluate the feasibility and applicability of the fusion technique across different satellite sensors. The TerraSAR-X dataset spans from August 2014 to March 2016, and the Sentinel-1 dataset from June 2015 to the end of 2017. Since the TerraSAR-X dataset has a spatial resolution of 3 meters, we applied a resampling process to align its PSInSAR grid results to a 15-meter resolution, ensuring spatial consistency in both resolution and PS point positioning with the Sentinel-1 dataset. The detailed temporal distribution of data can be found in Table 1 and Figure 6.

Table 1: PSInSAR dataset used for fusion

Satellite	Dataset	Start	End
Sentinel-1	Reference Dataset	2014/11/05	2017/12/19
Sentinel-1 Sentinel-1	Dataset 1	2014/11/05	2017/01/05
	Dataset 2	2016/01/11	2017/12/19
TerraSAR-X Sentinel-1	Dataset 1	2014/08/07	2016/03/01
	Dataset 2	2015/06/09	2017/12/19
GNSS	Validation	2014/08/01	2018/01/01

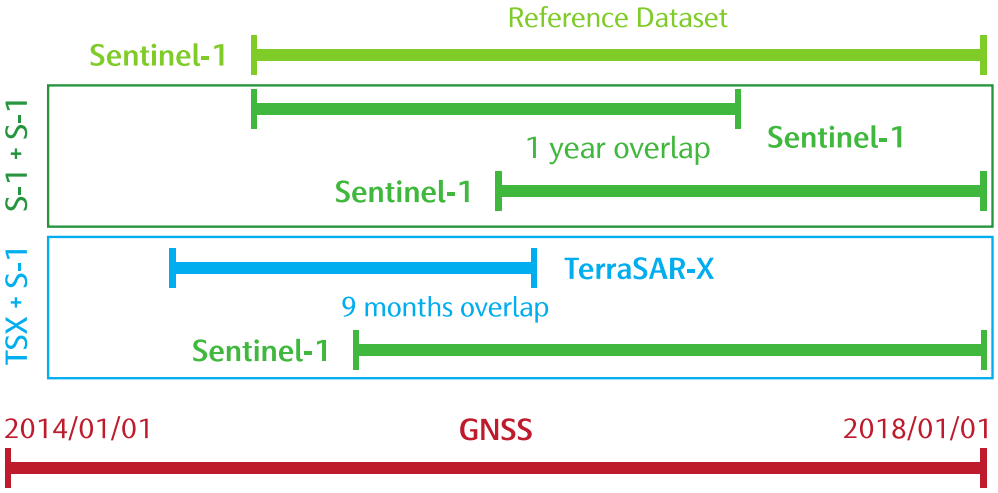

Figure 6: The illustration of PSInSAR datasets in the temporal domain.

Result and Discussion

We calculated the systematic offset between the two datasets, as shown in Figure 7. These values represent the amount that must be subtracted from Dataset 2 in subsequent analysis.

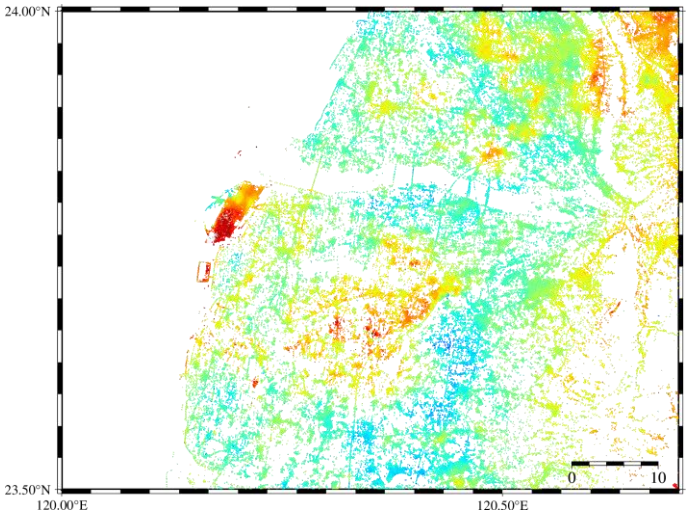

Figure 7: The bias between PSInSAR datasets obtained from continous PS.

To assign bias values to uncontinous PS pixels, we utilized the Triangulated Irregular Network (TIN) interpolation method to derive corresponding spatial offsets for further data processing. The interpolation results are shown in Figure 8. Based on these interpolation results, uncontinous PS in dataset 2 can subtract offset correction, allowing for the redefinition of the temporal reference point and the reconstruction of the time series.

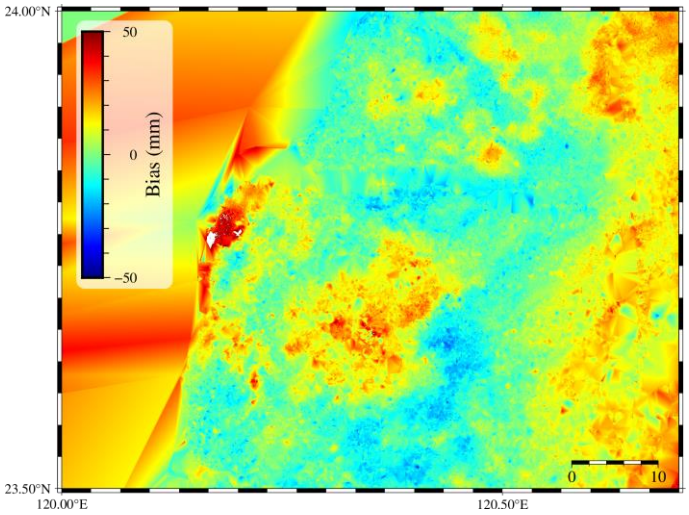

Figure 8: The interpolation results of bias.

Finally, we calculated the mean deformation velocity of the surface that integrates both continuous and uncontinous PS, as shown in Figure 9a. A comparison with fusion dataset with only continuous PS is shown in Figure 9b, where we observe that data for uncontinous PS has been successfully reserved. The PS count for Dataset 1 was 2,075,395, while for Dataset 2, it was 1,987,449. Using last year's continuous PS fusion technique, only 1,447,507 PS points were retained. However, the improved fusion technique developed this year yielded 2,614,902 PS points, including 1,167,395 uncontinous PS points.

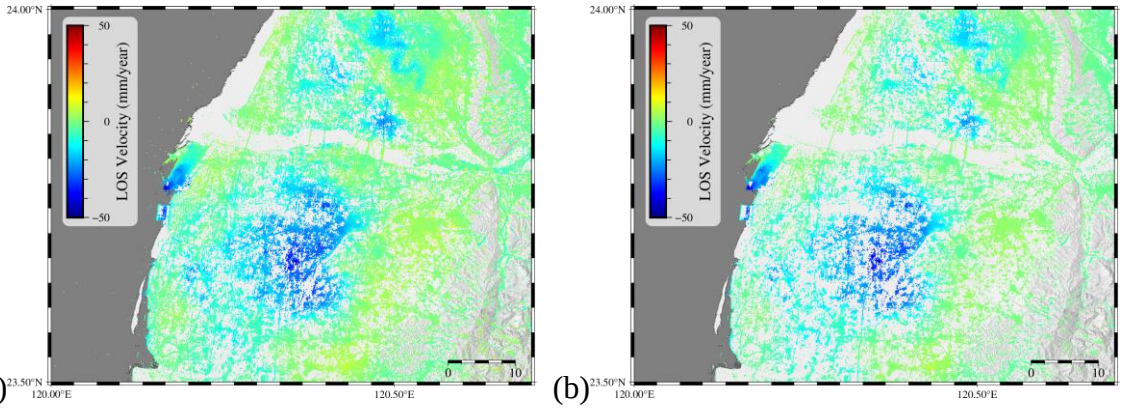

Figure 9: The PSInSAR fusion product (a) with all PSs (b) with only continous PS

To verify the accuracy of the fusion method developed in this study, we designed a two-stage data accuracy validation process. The first stage introduces GNSS observational data to assess the accuracy of the fused dataset. The second stage involves comparing the uncontinuous PS points in Dataset 2 to the reference dataset to determine if the time series of uncontinuous PS points with interpolated offsets aligns with the observation directly obtained from PSInSAR method. The reference dataset refers to the multi-temporal

deformation data generated directly from all Sentinel-1 data from November 2014 to December 2017 using the standard PSInSAR processing workflow. If the time series of uncontinuous PS points matches the observations in the original reference dataset, it indicates that the fusion technique produces results nearly identical to the original dataset, thereby validating the reliability of this fusion method for ultra-long-term multi-temporal PSInSAR applications and illustration.

We compared the trend of the fused dataset with GNSS data to see if they were consistent. A GNSS station HLES was selected in this step for time series analysis, and observational results from the reference dataset and the two datasets, before and after fusion, were compared. The time series of GNSS station HLES and the reference dataset are shown in Figure 10(a) The deformation time series of Datasets 1 and 2 are shown in Figure 10(b), where a consistency in the time series within the overlapping period can be observed, as well as a systematic offset between the two datasets. The fusion results, aligned with the GNSS time series, are presented in Figure 10(c). The fused dataset demonstrates a consistent result with the GNSS observation, indicating that the fused dataset accurately reflects the surface deformation.

(a)

(b)

(c)

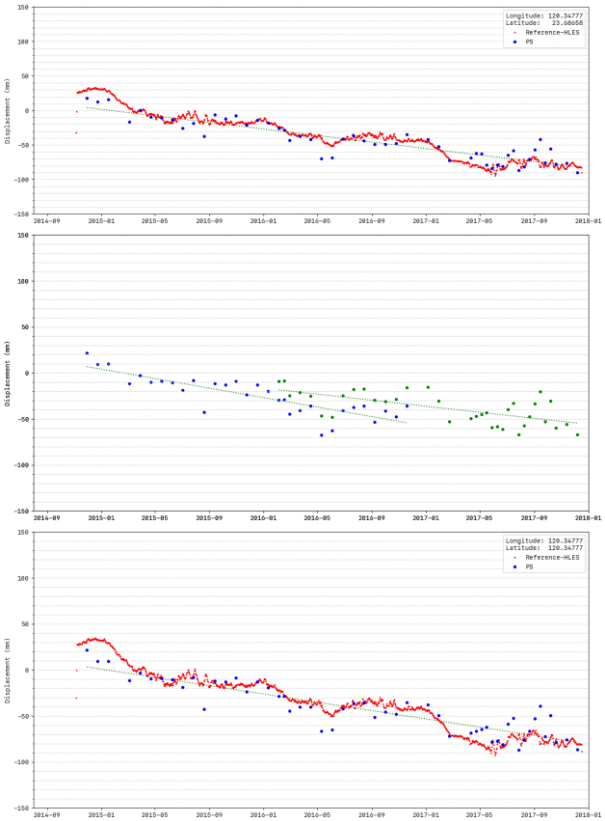

Figure 10: The time series of (a) reference dataset (b) dataset1 and 2 (c) fusion dataset.

To understand the differences between the fusion dataset and the GNSS / reference dataset, we calculated the average deformation values for PS points within a 100-meter radius

around every GNSS station in the study area. This average deformation value represents the PSInSAR observation results. We then compared the cumulative deformation values observed in the radar line-of-sight direction for each GNSS station with the cumulative deformation time series results from the PSInSAR fusion dataset. The results are shown in Figure 11(a), where the horizontal axis represents the cumulative deformation observed at each GNSS station at corresponding radar image times, and the vertical axis shows the cumulative deformation observed in the PSInSAR fusion dataset. As a result, a consistency between the two datasets, with a correlation coefficient of 0.85 and a root mean square error (RMSE) of 14.51 mm is observed. This result indicate that the fusion dataset is correlated with the GNSS observations, though the RMSE is slightly larger. For comparison, the reference dataset's correlation with GNSS observations can be also seen in Figure 11(b), with an identical correlation coefficient of 0.85 and an RMSE of 14.34 mm.

(a) (b) (c)

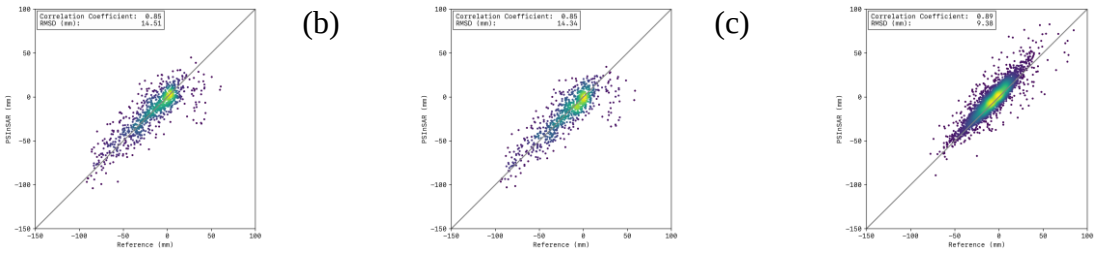

Figure 11: The comparison of accumulated deformation between (a) fusion dataset and GNSS (b) reference dataset and GNSS (c) fusion dataset and reference dataset

In the second phase of this study, we utilized imagery from both TerraSAR-X and Sentinel-1 satellites to perform dataset fusion, aiming to verify the feasibility and applicability of the fusion technique across different satellite sensors. The results of this fusion process are illustrated in Figure 12(a). Given the smaller spatial coverage of TerraSAR-X, the fusion method could only be conducted within the overlapping region of the two datasets. For comparison, the results obtained from the continuous PS are shown in Figure 12 (b). As a result, we obtained a total of 235,513 PS points. In contrast, the improved fusion technique developed in this study yielded 1,102,403 PS points, including 866,890 uncontinuous PS points. This significant increase in PS point density demonstrates the enhanced capability of the fusion method to reserve uncontinuous PS points, thereby facilitating a more comprehensive and robust deformation analysis.

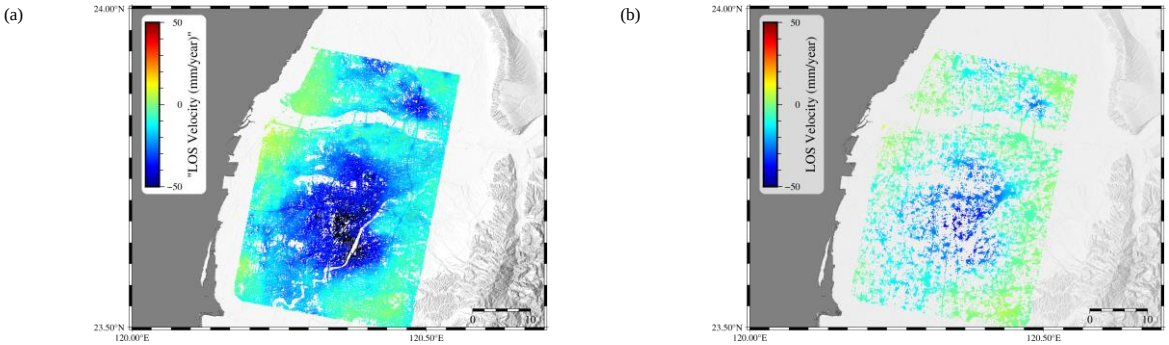

Figure 12: The PSInSAR fusion product (a) with all PSs (b) with only continous PS

We evaluate the accuracy of the PSInSAR fusion results by comparing them to GNSS station data. The results demonstrate a high level of consistency between the two datasets, with a calculated correlation coefficient of 0.82 and a root mean square error (RMSE) of 16.32 mm. This outcome indicates a correlation between the fusion dataset and GNSS observations. Additionally, we compared the time-series observations of uncontinuous PS points between the bridged dataset and the original reference dataset. The results are shown in Figure 13. The comparison indicates an agreement between the uncontinuous PS time-series observations in the fusion dataset and the reference dataset, with a correlation coefficient of 0.97. The RMSE for the differences between the two datasets is below 10 mm, which is within the typical precision range of PSInSAR observations.

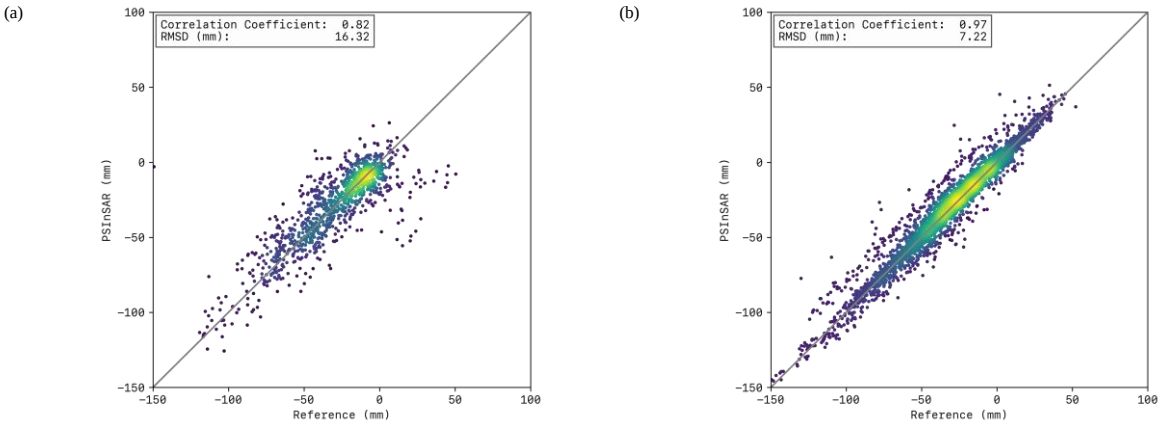

Figure 11: The comparison of accumulated deformation between (a) fusion dataset and (b) fusion dataset and reference dataset

Conclusion

In this study, the PSInSAR fusion method, aimed at integrating multiple datasets for extended multi-temporal surface deformation monitoring, is developed and validated. The results demonstrate that the proposed fusion technique achieves high accuracy in aligning

and combining deformation data from the same or different satellite sensors, even when variations in spatial resolution and observation periods are present.

By comparing the fused PSInSAR dataset with GNSS observations, we observed a consistency, with a correlation coefficient of 0.82 and a root mean square error (RMSE) of 16.32 mm. This high correlation indicates that the fused dataset accurately reflects the cumulative surface deformation trends observed by GNSS, which also confirms the reliability of the fusion process for long-term deformation monitoring.

Furthermore, the validation of uncontinuous PS points between the fused dataset and the reference dataset also showed promising results. The uncontinuous PS time-series observations achieved a correlation coefficient of 0.97 with the reference data, with an RMSE below 10 mm, which is within the accuracy range of PSInSAR techniques. This outcome confirms that the fusion method can provide a similar observation at those uncontinuous PS locations.

Finally, the fusion technique offers the capability to combine multi-source radar satellite images for multi-temporal radar differential interferometry surface deformation analysis. As a especially powerful technique for the GIS platform, end users will not need to know about SAR orbits, sensors, or the life period. They can get deformation anywhere and anytime if there are results in the database. Time series or mean velocity analysis across different time periods of various sensors is also possible. This approach provides an easy-to-use interface for surface deformation information to government agencies and private institutions for decision-making purposes.

Reference

Antonielli, B., Monserrat, O., Bonini, M., Righini, G., Sani, F., Luzi, G., ... & Aliyev, C. S., (2014), Pre-eruptive ground deformation of Azerbaijan mud volcanoes detected through satellite radar interferometry (DInSAR). Tectonophysics, 637, 163-177.

Chini, M., Atzori, S., Trasatti, E., Bignami, C., Kyriakopoulos, C., Tolomei, C., Stramondo, S., (2010), The May 12, 2008, (Mw 7.9) Sichuan Earthquake (China): Multiframe ALOS-PALSAR DInSAR Analysis of Coseismic Deformation. IEEE 、 GEOSCIENCE AND REMOTE SENSING LETTERS, VOL. 7, NO.

Huang, M. H., Tung, H., Fielding, E. J., Huang, H. H., Liang, C., Huang, C., & Hu, J. C., (2016), Multiple fault slip triggered above the 2016 Mw 6.4 MeiNong earthquake in Taiwan. Geophysical Research Letters, 43(14), 7459-7467.

Hooper, A., Zebker, H., Segall, P., & Kampes, B. (2004). A new method for measuring deformation on volcanoes and other natural terrains using InSAR persistent scatterers. Geophysical research letters, 31(23).

Le, T. S., Chang, CP., Nguyen X. T. and Yhokha A., (2016), TerraSAR-X Data for High-Precision Land Subsidence Monitoring: A Case Study in the Historical Centre of Hanoi, Vietnam. Remote Sens. 8(4), 338; doi:10.3390/rs8040338.

Luo, Q., Perissin, D., Lin, H., Zhang, Y., Wang, W., (2014), Subsidence monitoring of Tianjin suburbs by TerraSAR-X persistent scatterers interferometry. IEEE J. Sel. Top. Appl. Earth Obs. Remote Sens. 7, 1642–1650.

Massonnet, D., & Feigl, K. L. (1998). Radar interferometry and its application to changes in the Earth's surface. Reviews of geophysics, 36(4), 441-500.

Milillo, P., Bürgmann, R., Lundgren, P., Salzer, J., Perissin, D., Fielding, E., ... & Milillo, G. (2016). Space geodetic monitoring of engineered structures: The ongoing destabilization of the Mosul dam, Iraq. Scientific reports, 6, 37408.